INTERACTIVE RENDERING OF MULTIPLE SCATTERING IN PARTICIPATING MEDIA USING SEPARABLE PHASE FUNCTION

Zheng Gong, Zhimin Ren
State Key Laboratory of CAD&CG, Zhejiang University, Hangzhou, China

Zhangye Wang, Qunsheng Peng
State Key Laboratory of CAD&CG, Zhejiang University, Hangzhou, China

Keywords: Multiple scattering, participating media, phase function, singular value decomposition.

Abstract: This paper presents an interactive method to compute multiple scattering in non-homogeneous participating media with an effective phase function approximation. The volume is represented by grids, which allows us to render dynamic scenes. We achieve interactive computation rate by factorizing the phase function in transport equation with singular value decomposition (SVD) and keeping only the first few low-order approximation terms. These terms are paired 2D incident-direction texture maps and 2D outgoing-direction texture maps. The complicated integral calculation of in-scattering in each rendering pass is efficiently approximated by simply retrieving data from textures. Graphics hardware is also employed for on-the-fly computation. Using the proposed algorithm, we demonstrate rendering of multiple scattering in dynamic scenes at interactive rates.

1 INTRODUCTION

Realistic rendering in participating media has been a long standing and difficult problem in computer graphics. A detailed overview of rendering techniques in participating media can be found in (Cerezo, 2005). Back in the early 1990s, the Monte Carlo light tracing by (Pattanaik, 1993) uses a sampling process to calculate the points of absorption or scattering of the bundles within the volume. Later (Jensen, 1998) introduced photon mapping to volume containing photons in the participating media. Both of these methods can accurately simulate complicated lighting models. However, they are far from interactive. Nowadays, solution times with the fastest Monte Carlo approach still may take dozens of minutes.

Graphics hardware advanced rapidly in recent years, resulting in emergences of a great number of techniques that improve realism in near real-time. Most of the algorithms adopt simplified physics models or have constraints on media type. To name a few of these algorithms, (Harris, 2001) proposed a real-time cloud shading technique, but only multiple scattering in forward direction was precomputed. (Sloan, 2002) achieved interactively rendering multiple scattering assuming isotropic phase function and distant illumination. (Premože, 2004) provided a method that avoids direct numerical simulation of multiple scattering through spatial spreading. However, this approach only considered the overall statistics of the phase function, not its particular shape. (Hegeman, 2005) modified the previous method with hardware acceleration and achieved interactive rendering rates.

(Szirmay-Kalos, 2005) suggested a real-time method to compute multiple scattering in non-homogeneous participating media having general phase functions. This implementation adopted particle system and solved the transport equation iteratively with little simplification. Real-time performance was achieved by reusing light scattering paths that were generated with global line bundles traced in sample directions in a pre-processing phase. Nevertheless, once the particle moves, the light scattering paths have to be re-calculated, which is a time-consuming job. Thus, the volume is supposed to be static. In our paper, we

Gong Z., Ren Z., Wang Z. and Peng Q. (2007).
INTERACTIVE RENDERING OF MULTIPLE SCATTERING IN PARTICIPATING MEDIA USING SEPARABLE PHASE FUNCTION.
In *Proceedings of the Second International Conference on Computer Graphics Theory and Applications - GM/R*, pages 262-268
DOI: 10.5220/0002084002620268

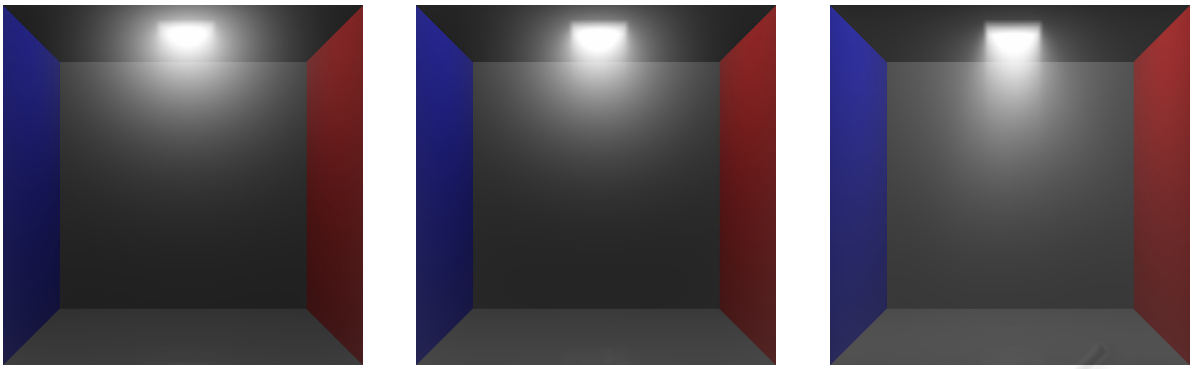

Figure 1: The appearance of participating media changes as the medium density is decreased from left to right. Multiple scattering appears distinctive in the image on the left and is less obvious in the one on the right. Results are produced by the proposed method at 2fps. The scene is illuminated by area light.

propose a method to solve the transport equation in volume represented by grids rather than particles. As a result, the calculation for the light scattering paths is avoided. With this approach, we realize rendering dynamic scenes.

Separable decomposition technique was introduced by (Kautz, 1999), and it has been used for BRDF rendering. Later (Wang, 2004) and (Liu, 2004) applied singular value decomposition (SVD) to glossy BRDFs in PRT. In addition, (Wang, 2005) introduced SVD to the approximation of BSSRDFs by separating Henyey-Greenstein (HG) phase function. Similarly, our proposed method decomposes HG phase function in the rendering of multiple scattering in participating media in order to accelerate the computation.

2 BACKGROUND

2.1 Multiple Scattering in Participating Media

When light travels in participating media, its radiance undergoes changes due to emission, in-scattering, absorption and out-scattering. The former two phenomena increase the radiance, while the latter two reduce it. The differential transport equation of radiance L in distance $d\vec{x}$ is:

$$\frac{dL(\vec{x},\omega_0)}{d\vec{x}} = \underbrace{\kappa_\alpha(\vec{x})L_e(\vec{x},\omega_0)}_{emission} - \underbrace{\kappa_\alpha(\vec{x})L(\vec{x},\omega_0)}_{absorption} \\ \underbrace{-\kappa_s(\vec{x})L(\vec{x},\omega_0)}_{out-scattering} + \underbrace{\frac{\kappa_s(\vec{x})}{4\pi}\int_\Omega L(\vec{x},\omega_i)p(\omega_0,\omega_i)d\sigma_{\omega_i}}_{in-scattering} \quad (1)$$

The increased radiance by ***emission*** can be expressed as $\kappa_\alpha(\vec{x})L_e(\vec{x})$, where $L_e(\vec{x})$ is the emission density, and $\kappa_\alpha(\vec{x})$ is the absorption coefficient, which is related to the density of participating media at point $\vec{x}$.

·***Absorption*** and ***out-scattering*** are respectively represented by $\kappa_\alpha(\vec{x})L(\vec{x})$ and $\kappa_s(\vec{x})L(\vec{x})$, where $L(\vec{x})$ is the radiance at point $\vec{x}$. $\kappa_s(\vec{x})$ is the scattering coefficient, and it is also related to density.

· ***In-scattering*** is due to photons originally moving in a certain direction being scattered into the considered direction. The number of scattered photons from differential solid angle $d\sigma_{\omega_i}$ equals to

$$\frac{\kappa_s(\vec{x})}{4\pi}\int_\Omega L(\vec{x},\omega_i)p(\omega_0,\omega_i)d\sigma_{\omega_i} \quad (2)$$

where $p(\omega_0,\omega_i)$ is the phase function. The phase function can be interpreted as the scattered intensity in direction ω_0, divided by the intensity that would be scattered in that direction if the scattering were isotropic (i.e. independent of the direction). Ω denotes the set of directions on the sphere around point $\vec{x}$.

The simplest phase function is the isotropic one. Rayleigh phase functions are used to model scattering processes produced by spherical particles whose radii are smaller than around one-tenth the light wavelength, while Mie phase functions are generally used when particle size is comparable to the radiation wavelength (Cerezo, 2005). In this paper, we take scattering in clouds and fog as examples, so the simple mathematical approximation of Mie phase functions, HG phase functions(Henyey, 1940)(Cornette, 1992), is used in our transport light model. The HG phase function is:

$$p(\theta) = \frac{1}{4\pi}\frac{1-g^2}{\left(1+g^2-2g\cos\theta\right)^{3/2}} \quad (3)$$

where $g \in (-1,1)$ is the media property describing how strongly the media scatters forward or backward, and θ denotes the angle between ω_i and ω_0.

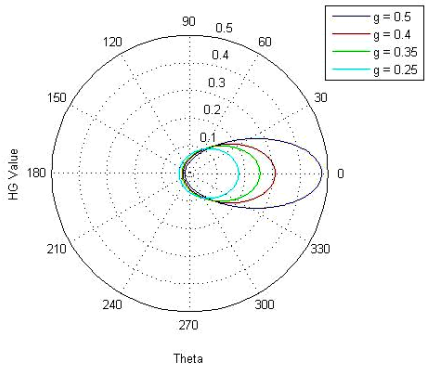

Figure 2: Phase Function (3).

The scattering properties of materials is depicted with the Figure 2, which is a plot of HG Phase function (3), where g is respectively 0.5, 0.4, 0.35, and 0.25.

2.2 Singular Value Decomposition (SVD) Factorization

In Mathematics, separable decompositions can approximate (to arbitrary accuracy) a high-dimensional function f with a sum of products of lower-dimensional functions g_k and h_k:

$$f(x,y) \approx \sum_{k=1}^{N} g_k(x) h_k(y) \tag{4}$$

Separable decompositions are usable for remarkably compressing the original function f when a good approximation can be found with a small N. In addition, they are capable of dividing variables into separate expressions, namely g_k and h_k. Further calculation which involves one variable may not need to refer to function f but to only one of the post-decomposition functions g_k or h_k instead. Redundant calculation can be avoided by adopting separable decompositions.

With the introduction of separable decomposition into pre-computing phase function in radiant Equation (1), the calculation speed is expected to be drastically enhanced. In this paper, we adopt the SVD method of decomposing phase function in order to considerably reduce the rendering time. We use SVD because it can produce relatively optimal approximations (Kautz, 1999). SVD of matrix A is the factorization that $A = USV^T$, where $U = [u_k]$, $V = [v_k]$ and $S = diag(\xi_k)$. S is a diagonal matrix of singular values ξ_k. As a result, after SVD, each function $f(x,y)$ can be approximated as:

$$f(x,y) \approx \sum_{k=1}^{N} \xi_k u_k(x) v_k(y) \cdot \tag{5}$$

3 THE PROPOSED METHOD

In this section, we elaborate our method for approximating transport equation using separable phase functions. We also present error estimation of our approximation compared with the original phase functions.

3.1 Discretization of the Transport Equation

The transport Equation (1) can be discretized into the form

$$\begin{aligned} \frac{dL(\vec{x},\omega_0)}{d\vec{x}} &\approx \underbrace{\kappa_\alpha(\vec{x}) L_e(\vec{x},\omega_0)}_{emission} \\ &- \underbrace{\kappa_\alpha(\vec{x}) L(\vec{x},\omega_0)}_{absorption} - \underbrace{\kappa_s(\vec{x}) L(\vec{x},\omega_0)}_{out-scattering} \\ &+ \underbrace{\frac{\kappa_s(\vec{x})}{4\pi} \frac{4\pi}{D} \sum_{d=1}^{D} L(\vec{x},\omega_d) p(\omega_0,\omega_d)}_{in-scattering} \end{aligned} \tag{6}$$

where D is the number of sample directions. The above equation can be solved by iterations. Suppose at iteration step n, we have the light radiance $L^n(\vec{x})$, the light radiance of step $n+1$ can be obtained after one iteration:

$$\begin{aligned} L^{n+1}(\vec{x}+d\vec{x},\omega_0) &\approx L^n(\vec{x},\omega_0) + \\ &\underbrace{\kappa_\alpha(\vec{x}) L_e(\vec{x},\omega_0) d\vec{x}}_{emission} - \underbrace{\kappa_t(\vec{x}) L^n(\vec{x},\omega_0) d\vec{x}}_{out-scattering\,\&\,absorption} \\ &+ \underbrace{\frac{\kappa_s(\vec{x})}{4\pi} \frac{4\pi}{D} \sum_{d=1}^{D} L^n(\vec{x},\omega_d) p(\omega_0,\omega_d) d\vec{x}}_{in-scattering} \end{aligned} \tag{7}$$

where $\kappa_t(\vec{x}) = \kappa_\alpha(\vec{x}) + \kappa_s(\vec{x})$. For physically visible materials, this iteration is convergent.

3.2 Separable Phase Function and Error Estimation

3.2.1 Factorizing the Phase Function

In the general phase function $p(\omega_0,\omega_i)$, ω_0 represents the incident light, and ω_i is the arbitrary outgoing light. We can sample the D directions in the whole direction space and construct a $D \times D$ matrix A. Each element in column ω_0 and row ω_i of A represents the value of $p(\omega_0,\omega_i)$. We apply SVD on A and obtain:

$$p(\omega_0,\omega_i) \approx \sum_{k=1}^{N} \xi_k u_k(\omega_0) v_k(\omega_i). \tag{8}$$

SVD approximates the multivariate phase function $p(\omega_0,\omega_i)$ as a sum of products of functions

u_k and v_k of lower dimensionality. In Equation (8), N is the number of terms used in approximation. By this approach, phase function is divided into two parts $u_k(\omega_0)$ and $v_k(\omega_i)$, which are only pertinent with ω_i and ω_0 respectively. Consequently, the phase function is approximated by a few low-order terms. Each of them can be represented by a 2D texture map $\sqrt{\xi_k}u_k(\omega_0)$ or $\sqrt{\xi_k}v_k(\omega_i)$ respectively indexed by the incident direction ω_0 or an outgoing direction ω_i in Ω. We name $\sqrt{\xi_k}u_k(\omega_0)$ incident-direction map and $\sqrt{\xi_k}v_k(\omega_i)$ outgoing-direction map.

We observe that $p(\omega_0,\omega_i)$ only varies with the angle between ω_0 and ω_i, so A should be real symmetric. Symmetric matrix A can be diagonalized into the form $A=QMQ^T$, where diagonal element of M are the eigenvalues of A, and the column vectors of Q are the corresponding eigenvectors. As described in Section 2.2, matrix A can be factorized with SVD into $A=USV^T$. In this case, $U=V=Q$ and $S=M$, so $\sqrt{\xi_k}u_k(\omega_0)$ and $\sqrt{\xi_k}v_k(\omega_i)$ should only differ by the sign.

After applying SVD to the phase function, the iterative transport equation is transformed into,

$$\begin{aligned} L^{n+1}(\vec{x}+d\vec{x},\omega_0) &\approx L^n(\vec{x},\omega_0) \\ &+ \underbrace{\kappa_a(\vec{x})L_e(\vec{x},\omega_0)d\vec{x}}_{emission} - \underbrace{\kappa_t(\vec{x})L^n(\vec{x},\omega_0)d\vec{x}}_{out-scattering\&absorption} \\ &+ \underbrace{\frac{\kappa_s(\vec{x})}{4\pi}\frac{4\pi}{D}\sum_{k=1}^{N}\sqrt{\xi_k}u_k(\omega_0)\sum_{d=1}^{D}L^n(\vec{x},\omega_d)\sqrt{\xi_k}v_k(\omega_d)d\vec{x}}_{in-scattering} \end{aligned} \quad (9)$$

3.2.2 Error Estimation of SVD Approximation

SVD can be applied to general phase functions, and the approximation can be arbitrarily accurate. We are going to demonstrate the result of our approximation of phase functions with cloud rendering. In this case, HG phase functions (Equation (3)), are most frequently adopted. Therefore, we present the root mean squared error (RMES) of SVD approximation for HG phase functions here. We apply SVD to HG phase functions and obtained the RMES, which is shown in Figure 3.

From the bellow figure, the approximation takes greater number of terms to achieve certain accuracy as g grows. The RMSE of SVD is about 10% for approximations of 24 terms when g equals 0.5. It is a numerically acceptable approximation, and it is used for cloud rendering in this paper.

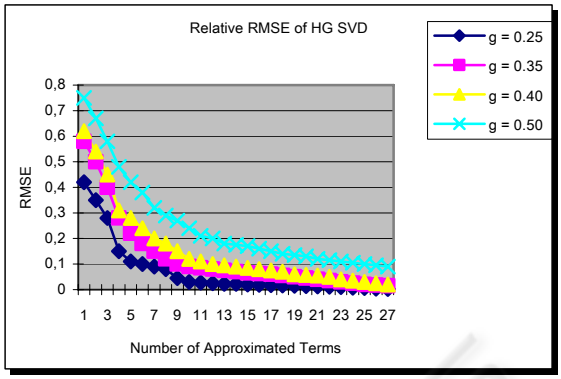

Figure 3: Relative RMSE of HG SVD.

4 IMPLEMENTATION

4.1 Precomputation

We use the software MATLAB for precalculating the SVD results of phase functions. The incident-direction map $\sqrt{\xi_k}u_k(\omega_0)$ and outgoing-direction map $\sqrt{\xi_k}v_k(\omega_i)$ are precomputed and respectively stored in textures: Incident-Direction Texture and Outgoing-Direction Texture. Both of them are 2D textures indexed by column number $k\in(1,N)$ and row number $i\in(1,D)$

In Figure 4, we plotted the original HG phase function values and the approximated HG phase function values after applying SVD, using 8 and 24 approximating terms respectively.

4.2 Runtime Rendering Pipeline

We represent our grids with what is called a flat 3D texture (Harris, 2003). A flat 3D texture represents actually a 3D volume, as shown in Figure 5. Flat 3D textures can be updated in a single rendering pass.

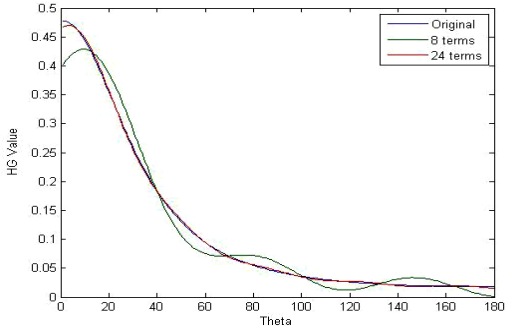

Figure 4: Original HG Phase Function and SVD-Approximated HG Values Plotted Using 8 and 24 Terms.

This means that a 3D simulation can be implemented in the same number of passes as that required by an equivalent 2D simulation. Thus, it provides a quick and inexpensive way to perform 3D simulation.

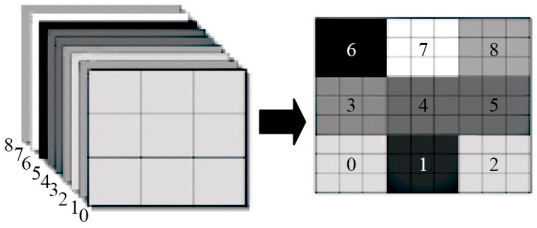

(a) (b)

Figure 5: 3D texture (a) and its corresponding flat 3D texture (b).

This section presents the rendering pipeline with hardware acceleration during runtime. In every pass of fragment program, we input Density Texture, Radiance Texture, Incident Texture and Outgoing Texture at iteration step n to update the values of step $n+1$. The Density Texture and the Radiance Texture respectively contain the density and radiance values at each point in the rendering volume. The Incident Texture indexes $\sqrt{\xi_k}u_k(\omega_0)$ with k, and the Outgoing Texture contains the value of

$$\sum_{d=1}^{D} L^n(\vec{x},\omega_d)\sqrt{\xi_k}v_k(\omega_d) \tag{10}$$

for each k at each point. The rendering pipeline at runtime is illustrated in Figure 6.

For each iteration, the process runs through the fragment program a number of D times. During each pass of fragment program, the radiance $L^{n+1}(\vec{x}+d\vec{x},\omega_0)$ in direction $d\in(1,D)$ is updated with Equation (9), and

$$\sum_{k=1}^{N}\sqrt{\xi_k}u_k(\omega_0)\sum_{d=1}^{D}L^n(\vec{x},\omega_d)\sqrt{\xi_k}v_k(\omega_d)d\vec{x} \tag{11}$$

is also calculated. $\sqrt{\xi_k}u_k(\omega_0)$ is indexed from Incident Texture, and

$$\sum_{d=1}^{D} L^n(\vec{x},\omega_d)\sqrt{\xi_k}v_k(\omega_d)d\vec{x} \tag{12}$$

is indexed from Outgoing Texture. In this way, the original integral calculation:

$$\sum_{d=1}^{D} L(\vec{x},\omega_d)\,p(\omega_0,\omega_d) \tag{13}$$

in Equation (9) is avoided by simply retrieving values from a texture.

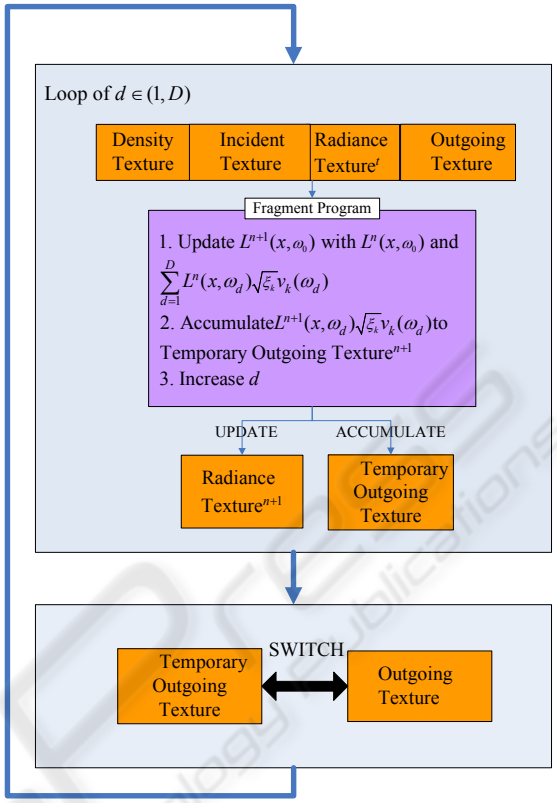

Figure 6: Implementation Pipeline.

It remarkably reduces required calculation amount during every rendering pass, thus the rendering speed is considerably increased. At the same time,

$$L^{n+1}(\vec{x},\omega_d)\sqrt{\xi_k}v_k(\omega_d) \tag{14}$$

is added to the Temporary Outgoing Texture for each $k\in(1,N)$, and d is increased afterwards. When d reaches D, an iteration is complete. Thus $L^{n+1}(\vec{x},\omega_0)$ in all D directions has been updated. Meanwhile, the value of each grid in the Temporary Outgoing Texture has been updated to be

$$\sum_{d=1}^{D} L^{n+1}(\vec{x},\omega_d)\sqrt{\xi_k}v_k(\omega_d) \tag{15}$$

Temporary Outgoing Texture and the Outgoing Texture are switched for the next iteration. Iteration continues, and eventually $L^{n+1}(\vec{x},\omega_0)$ differs little with $L^n(\vec{x},\omega_0)$, which indicates the convergence of iteration.

20 iterations 40 iterations 60 iterations

Figure 7: A cloud illuminated at sun set. The images show appearances of the cloud with different iteration steps.

5 RESULTS AND DISCUSSIONS

The proposed technique has been implemented in Direct3D/HLSL environment and run on an NV7800GT graphics card. The volume resolution is $64 \times 64 \times 64$.

In Figure 1, we demonstrate the appearance of multiple scattering in participating media with different uniform densities. The scene is illuminated with parallel light rays travelling downwards from a window in the ceiling. The number of discrete directions, D, is 128. The albedo is 0.9. The multiple scattering is more representative in medium with a larger density, while single scattering dominates the scene of smaller density. We compute one iteration in each frame, and when the uniform density changes, we take the solution of the previous frame as the initial value of the iteration, which results in fast convergence. The scene is simulated as 2fps. A dynamic scene is rendered interactively.

In Figure 7, we follow the converging process of a piece of cloud after different iteration steps. The image on the left displays the cloud after 20 iterations. At that time, the part closer to the sun is firstly illuminated. In the images in the middle, the energy gradually transports to other parts of the cloud. Notice that the thicker part of the cloud appears darker because of high extinction. The image on the right shows the final stable appearance of the cloud, which indicates the convergence of transport equation. The number of discrete directions D is 256, and 1.5fps was achieved.

In Figure 8, we present an example of HG phase function factorized by SVD. The image on the left is rendered without factorizing the phase function. On the right is an image shaded with our method, using 24-term SVD approximation. g is 0.5 in both simulations. From the comparison, the cloud appears a little darker in our proposed model, especially in the thick part. It is due to that the reconstructed value of the phase function with our method is generally smaller than the original one, and phase function is only related to the in-scattering part of the transport equation. Therefore, the approximated in-scattering energy is smaller than the actual value. However, a rendering speed of 1.5fps is achieved with the proposed algorithm compared with 0.2fps of the unfactorized model. Moreover, visually good results are obtained by the approximation. With our approach, rendering speed is considerably enhanced, while realism is mostly preserved.

Original N = 24

Figure 8: SVD factorization example, illuminated by the sun.

6 CONCLUSIONS

We have presented a method for interactively rendering multiple scattering in participating media with little physics simplification and constraints on media type. Compared with the Monte Carlo rendering method, our approach achieves much higher rendering speed. Meanwhile, compared with other near real-time algorithms, such as (Harris, 2001) and (Sloan, 2002), ours has little constraints on the lighting conditions. The material properties and the scattering phase function. We approximate phase functions in transport equation with singular value decomposition. Using the proposed algorithm, rendering of dynamic scenes can be implemented with grid system. This technique greatly reduces the required calculation amount and enhances the

rendering speed. The proposed method successfully models dynamic scenes that do not change rapidly.

However, as to highly dynamic scenes, the transport equation takes more time to converge. Once the change occurs before the convergence, error appears and accumulates successively.

Therefore, we plan to focus on developing a better model which converges faster in future work.

ACKNOWLEDGEMENTS

This research is supported by 973 program of China under grant 2002CB312101, the National Natural Science Foundation of China under grant 60603076 and 60475013.

REFERENCES

Cerezo, E., Pérez, F., Pueyo, X., Seron, F. J., Sillion, F. X., 2005. A Survey on Participating Media Rendering Techniques. In *The Visual Computer 21,* pp. 303-328, 2005.

Cornette W., Shanks J., 1992. Physical reasonable analytic expression for single-scattering phase function. *Applied Optics 31*, 16, 31–52, 1992.

Harris, M. J., Lastra, A., 2001. Real-Time Cloud Rendering. In *Proceedings of Eurographics 2001,* 20(3):76-84, September 2001.

Harris, M. J., Baxter W. V. III, Scheuermann T., Lastra A.. Simulation of Cloud Dynamics on Graphics Hardware. In *Proceedings of Graphics Hardware 2003*.

Hegeman, K., Ashikhmin, M., Premoze, S., 2005. A Lighting Model for General Participating Media. In *Proceedings of ACM SIGGRAPH Symposium on Interactive 3D Graphics and Games*, April 2005.

Henyey, G., Greenstein, J., 1940. Diffuse radiation in the galaxy. *Astrophysical Journal 88*, 70–73, 1940.

Jensen, H. W., Christensen, P. H., 1998. Efficient simulation of light transport in scenes with participating media using photon maps. In *Proceedings of ACM SIGGRAPH 98,* 311--320.

Kautz, J., McCool, M., 1999. Interactive Rendering with Arbitrary BRDFs using separable approximation. In *10th Eurographics Workshop on Rendering, 1999*, pp. 255-268, 379 (colour plate).

Liu, X., Sloan, P.-P., Shum, H.-Y., Snyder, J., 2004. All-Frequency Precomputed Radiance Transfer for Glossy Objects. In *Eurographics Symposium on Rendering* 2004, pp.337-344, 2004.

Pattanaik, S. N., Mudur, S. P., 1993. Computation of Global Illumination in a Participating Medium by Monte Carlo Simulation. In *The Journal of Visualization and Computer Animation,* 4(3):133–152, July - September 1993.

Premože, S., Ashikhmin, M., Tessendorf, J., Ramamoorthi, R., Nayar, S., 2004. Practical rendering of multiple scattering effects in participating media. In *Proceedings of the Eurographics Symposium on Rendering* 2004.

SLOAN, P.-P., KAUTZ, J., SNYDER, J., 2002. Precomputed radiance transfer for real-time rendering in dynamic, low-frequency lighting environments. In *ACM Transactions on Graphics* 21, 3 (July), 527–536.

Szirmay-Kalos, L., Sbert, M., Ummenhoffer, T., 2005. Real-Time Multiple Scattering in Participating Media with Illumination Networks. In *Proceedings of the Eurographics Symposium on Rendering* 2005.

Wang, R., Tran, J., Luebke, D., 2004. All-frequency relighting of non-diffuse objects using separable BRDF approximation. In *Proceedings of Eurographics Symposium on Rendering* 2004, pp.345–354, 2004.

Wang, R., Tran, J., Luebke, D., 2005. All-frequency interactive relighting of translucent objects with single and multiple scattering. In *ACM Transactions on Graphics*, 24(3): 1202-1207.